



Restoration of Degraded Calcium-Silicate-Hydrate in Calcium-Leached Cement Paste

Thinh Nguyen^{1,2} , Quoc Tri Phung¹ , Norbert Maes¹, Geert De Schutter³, and Özlem Cizer²

¹ Belgian Nuclear Research Center, Boeretang 200, 2400 Mol, Belgium
luong.the.thinh.nguyen@sckcen.be

² KU Leuven, Kasteelpark Arenberg 40, 3001 Leuven, Belgium

³ Ghent University, Technologiepark-Zwijnaarde 60, 9052 Gent, Belgium

Abstract. Calcium leaching, a degradation process of cementitious materials, is a major concern in nuclear waste disposal facilities. Leached materials experience a drop in pH, dissolution of portlandite and degradation of other hydrated phases leading to a coarse microstructure, and thereby higher transport properties. Despite the fact that the mechanism and consequences of calcium leaching have been widely studied in the literature, little to no study has been done to evaluate the potential of reversing this process.

The goal of this research is to investigate a structural repair process termed “recalcification”, which has a potential to reverse part of the calcium leaching, restoring the phase composition and structure of the deteriorated cementitious materials. CEM I cement paste with water/cement ratio of 0.5 was casted and cured for 48 days in sealed plastic tubes. Smaller specimens of size $D \times H = 10 \times 7$ mm were then leached in NH_4NO_3 6M for 24 h before being immersed in a bath of saturated $\text{Ca}(\text{OH})_2$ for recalcification. After 6 days, samples were freeze-dried and characterized with phenolphthalein spraying, FTIR, MIP and SEM-EDX.

The results show that after recalcification, the Ca/Si ratio of the leached zone increases as the silicate chain length of C-S-H decreases. In the pores formed by leaching, a formation of web-like network of C-S-H is observed. As a result, the pore size distributions of recalcified samples shift from larger to smaller sizes, demonstrating the pore-filling effect during recalcification.

Keywords: Recalcification · Leaching · C-S-H · Ca/Si ratio · Pore size distribution

1 Introduction

Calcium leaching is one of the degrading processes that leads to the loss of mechanical properties, microstructure, and macrostructure of cementitious materials [1]. Calcium leaching is the process of removing calcium ions from a cementitious matrix and transferring them into the external environment. Depending on their solubility, calcium leaching can impact all hydrated phases. However, its effects on calcium-silicate-hydrate (C-S-H) and portlandite (CH) are of the utmost importance, as these are the primary cement hydration products.

Due to its high relatively high solubility compared with other Ca-bearing hydrates, calcium leaching begins with CH upon contact with the leachant. As CH dissolves, capillary pores begin to expand, which ultimately leads to the loss of elasticity [2]. In contrast to the simple dissolving of CH, the calcium leaching of C-S-H follows a very complicated pathway. In C-S-H, calcium ions exist as Ca-OH on the surface, Ca-O-Si linking the C-S-H chains, and Ca-O as the building block of each layer [3, 4]. Interlayer Ca-O-Si begins to dissolve at approximately Ca/Si 1.2, whereas intralayer Ca-O dissolves around Ca/Si 0.7 [4, 5]. Following the elimination of inter and intralayer calcium, Si-OH is polymerized to create Si-O-Si, releasing water in the process. According to the literature, the polymerization of silicate chains is the primary source of leaching shrinkage [6]. As leaching continues, C-S-H then completely decomposes into silica gel, leading to a complete disintegration of the cement paste.

Calcium leaching happens in nature wherever there is water, acid, or nitrate ions. The kinetics of natural leaching are fairly slow (2.3 mm a year in water [7, 8]), hence accelerated leaching is used in a laboratory setting to simulate longer periods of degradation. NH_4NO_3 is a common choice for accelerated leaching, as it provides hundreds of times quicker leaching than leaching in water while retaining the same leaching mechanism [7]. Some studies have reported the formation of the expansive calcium nitro-aluminate phase due to the reaction between $\text{Ca}(\text{NO}_3)_2$ and hydrated aluminates [7, 9]. This phase should however remain in a soluble form [9] since our experiments were carried out under full immersion in the NH_4NO_3 solution.

Even though calcium leaching has been extensively explored in the literature, very little research has been conducted on the prospect of reversing the process, with the exception of the work of Chen et al. [3], in which a $\text{Ca}(\text{OH})_2$ solution was added to a leached C_3S paste with a Ca/Si ratio of 0.83 to produce one with a Ca/Si ratio of 1.31. However, no additional research was conducted on microstructural alterations.

The purpose of this study is to investigate the reversibility of calcium leaching and the impacts of the restoration - recalcification. Changes in the pore structure of leached and recalcified CEM I specimens were examined using Scanning Electron Microscopy (SEM) and Mercury Intrusion Porosimetry (MIP), whereas Ca/Si was quantified using Energy Dispersive X-Ray analysis (SEM-EDX). Fourier-transformed Infrared Spectroscopy (FTIR) was used to detect changes in the degree of polymerization of silicate chains. The pH shift caused by calcium leaching and recalcification was visualized by spraying phenolphthalein. Finally, the prospect of employing recalcification as a repair technique is discussed in the following sections.

2 Experiments

2.1 Sample Preparation

Cement paste samples were made from CEM I 52.5N cement and its chemical compositions are detailed in [10]. At a water-to-cement ratio of 0.5, cement powder was hand-blended with tap water. The mixture was then allowed to cure in sealed 10-mm-wide plastic tubes inside a temperature-controlled chamber at 20 ± 01 °C. After 48 days, 7-mm-thick samples were sawn from tubes of cured cement. A set of references was packed in a plastic bag for the same duration as calcium leaching and freeze-dried alongside samples that had been leached.

2.2 Calcium Leaching in NH_4NO_3

Since the leaching test was designed to occur from the two freshly cut surfaces (for ease to develop a 1D model – not presented in this paper), PVC adhesive was added to the samples' rims to prevent leaching from the sides. Figure 1 provides an illustration of the sample preparation. The leaching procedure was adapted from other authors [11, 12]. To guarantee thorough dissolution of NH_4NO_3 crystals, a 6M NH_4NO_3 solution was prepared the day before use (VWR). To eliminate the presence of undesirable ions, deionized (DI) water was utilized to make the solution.

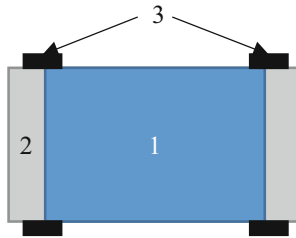
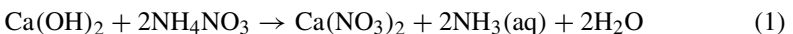
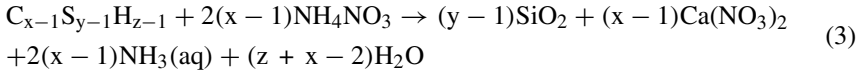
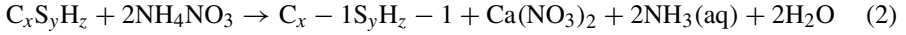


Fig. 1. Sketching of a sample encased by PVC tube, with the rims sealed by PVC adhesive: (1) cement paste, (2) PVC tube, (3) PVC adhesive.

Cement paste leaching in NH_4NO_3 generates NH_3 according to Eqs. (1), (2), (3) [11]. In order to proceed with the leaching process, it was necessary to evacuate the created NH_3 gas. For that purpose, leaching was carried out in a sealed glass container with constant low N_2 flow. To guarantee the uniformity of the NH_4NO_3 concentration, the NH_4NO_3 solution was stirred using a magnetic stirrer. An adequate amount of NH_4NO_3 equal to eight times the entire contact surface area of samples was used to avoid the renewal of the leachant [11]. After 24h of leaching, samples were submerged in DI water to remove NO_3^- and unreacted NH_4^+ from pore solution. Then, the samples were freeze-dried (immersion in liquid N_2 , followed by drying at 0.1 mbar for 24h) and stored in sealed plastic bags with silica gel.





2.3 Recalcification in Ca(OH)₂ Solution

Half of the leached specimens were placed in a plastic chamber filled with a saturated Ca(OH)₂ solution. Ca(OH)₂ powder (VWR, analytical grade, 95 percent) was mixed with DI water to make the saturated Ca(OH)₂ solution. After that, the supernatant was collected and utilized for recalcification. On a rotating plate, recalcification was allowed to occur for 6 days. The recalcified samples were then freeze-dried (immersion in liquid N₂, followed by drying at 0.1 mbar for 24 h) for further analysis.

2.4 Characterizations

Phenolphthalein Spray

After freeze drying, the leached and the recalcified samples were sliced in half perpendicular to the leaching surface. On the freshly sliced surfaces, 0.5 percent phenolphthalein in ethanol was applied sparingly. Photos of phenolphthalein-sprayed samples were taken immediately. The samples were then packed in containers with silica gel and preserved for further use.

FTIR

FTIR allows for observation of the Si-O vibration, symbolic of the polymerization of silicate chains. Samples were measured in mid-IR, utilizing an ATR module with a resolution of 1 cm⁻¹ and an average of 100 scans. Powder for FTIR measurements was collected by scratching the deteriorated zone (~1.5 mm in thickness) on the freshly cut surfaces of samples.

The baseline shift caused by scattering in the obtained spectra was then corrected using the software SpectraGryph. The Si-O asymmetric stretching peaks ν_3 (in polymeric unit of [SiO₄]⁴⁻) at 940–980 cm⁻¹ of reference, leached, and recalcified samples were equalized in height in order to illustrate peak shifting more effectively.

MIP

For the measurement of MIP, about 1 g of freeze-dried samples were loaded into a dilatometer. The MIP instrument is comprised of two smaller components: a lower pressure unit, Pascal 140, with a maximum pressure of 200 kPa, and a higher pressure unit, Pascal 440, with a maximum pressure of 400 MPa. Since the pressure of 200 MPa

is enough to reach the gel pores (nm sizes), such pressure was chosen in this study. The acquired intrusion data were further analyzed and plotted in Origin.

SEM and EDX

Flat, resin-embedded samples were required for the EDX measurement, thus specimens were immersed in epoxy resin before being cut in half perpendicular to the leaching/recalcification surfaces. To achieve a smooth finish, the freshly cut surfaces were re-impregnated and polished. To avoid charge buildup, a thin layer of gold with a thickness of approximately 10 nm was coated in Argon onto the surface before measuring. The samples were measured in a Phenom tabletop SEM with a magnification of $500\times$ and a beam power of 15 kV. The Ca/Si ratios were mapped using the Phenom SEM's EDX module. On each sample, two lines were scanned for average, beginning at the contact surface and progressing to a depth of 2.5 mm. Spraying phenolphthalein on the intersection yielded an estimate of the depth value. The measured Ca/Si ratios were corrected using minerals with known chemical compositions.

Morphology of the C-S-H network was captured on rough-surfaced samples under SEM. The surfaces of interest were coated with 10 nm of gold in Argon prior to measurements.

3 Results and Discussions

3.1 Chemical Alteration Due to Calcium Leaching and Recalcification

Calcium leaching removes calcium ions from the cement matrix, lowering the pH of the affected area. As a pH indicator, phenolphthalein is often used to visually check the pH-lowering effect of leaching. The phenolphthalein-sprayed surfaces are displayed in Fig. 2. After 24 h of immersion in NH_4NO_3 6M, a pink-less zone appears, which is considered the deteriorated zone (Fig. 2b). Since the range of color shifting of phenolphthalein lies at pH from 8.3 to 10.0 [13], the colorless region indicates a pH value lower than 10, or a total removal of CH and partial leaching of C-S-H. The corresponding deteriorated zone is shown in pink on Fig. 2a. The pink color suggests a pH greater than 10 and an increase in calcium concentration in that zone. The increased calcium content comes from the saturated $\text{Ca}(\text{OH})_2$ solution used in recalcification; however one might question whether the extra calcium incorporates into the cement matrix or just remains in the pore solution. Because the solution employed in this study is not supersaturated, there should be no expectation of newly produced CH as a result of recalcification.

Even though no new CH is formed in the recalcified samples, calcium from the external $\text{Ca}(\text{OH})_2$ solution undoubtedly integrates into the cement matrix, as evidenced by SEM-EDX calcium and silicon measurements (Fig. 3). Unlike the reference, which has a Ca/Si ratio that fluctuates about 2 across the sample, the Ca/Si ratio of leached and recalcified samples rises with increasing distance from the contact surface. We notice that the Ca/Si curve of leached OPC behaves strangely at the distance region between 1.6 mm and 2.5 mm. It might be attributed to the fact that there are only two EDX scans per sample and that the centre of the sample has more crystals than the deteriorated zone. Nevertheless, the increased Ca/Si ratios in the first 1 mm, or the degraded zone, is further confirmed by FTIR data.

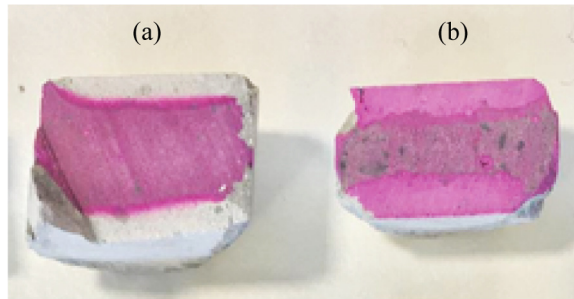


Fig. 2. Phenolphthalein-sprayed leached (a) and recalcified (b) cement paste.

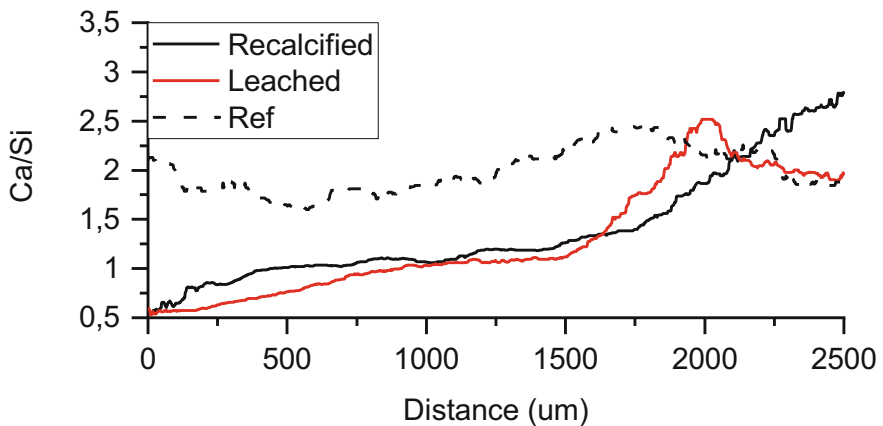


Fig. 3. Ca/Si ratio from the contact surface to the depth of 2.5 mm.

3.2 Microstructure Alteration Due to Calcium Leaching and Recalcification

The FTIR vibration of the Si-O bond in $[\text{SiO}_4]^{4-}$ tetrahedral is shown in Fig. 4. The Si-O ν_3 stretching mode produces a peak about $950\text{--}970\text{ cm}^{-1}$. As a result of leaching, silicate chain polymerization is anticipated to shift the position of the Si-O stretching peak to the blue (higher wavenumber). Figure 4 depicts a 10 cm^{-1} change from 952 cm^{-1} on the reference line to 962 cm^{-1} . Calcium leaching removes calcium from the Si-O-Ca bond, resulting in the formation of Si-OH. Polymerization is the process of lengthening a silicate chain by joining two Si-OH bonds and releasing a water molecule. Polymerization of the silicate chain has been linked to shrinkage, pointing to polymerization as the primary source of shrinkage and cracking [6]. Because C-S-H can be produced by mixing SiO_2 and $\text{Ca}(\text{OH})_2$ in water, where Ca^{2+} interacts with and breaks the Si-O-Si and Si-OH bonds, recalcification should operate similarly. In Fig. 4, the Si-O peak of the recalcified sample can be seen shifting to the red, to 956 cm^{-1} , from 952 cm^{-1} on the leached sample. The red shift of the Si-O stretching peak suggests that the Si-O bonds in $[\text{SiO}_4]^{4-}$ groups are weakened. The weakening implies a chemical incorporation of Ca^{2+} cations from $\text{Ca}(\text{OH})_2$ solution into the deteriorated C-S-H gel, breaking some

Si-O-Si bonds to yield Si-O-Ca. The durations of leaching (1 day) and recalcification (6 days) shows that the rate of recalcification in $\text{Ca}(\text{OH})_2$ is slower than that of leaching in NH_4NO_3 . Recalcification in $\text{Ca}(\text{OH})_2$ is understandably slower, especially given that calcium leaching in NH_4NO_3 is hundreds of times quicker than leaching in water. For better comparison, the rate of recalcification should be compared to the rate of calcium leaching in pure water.

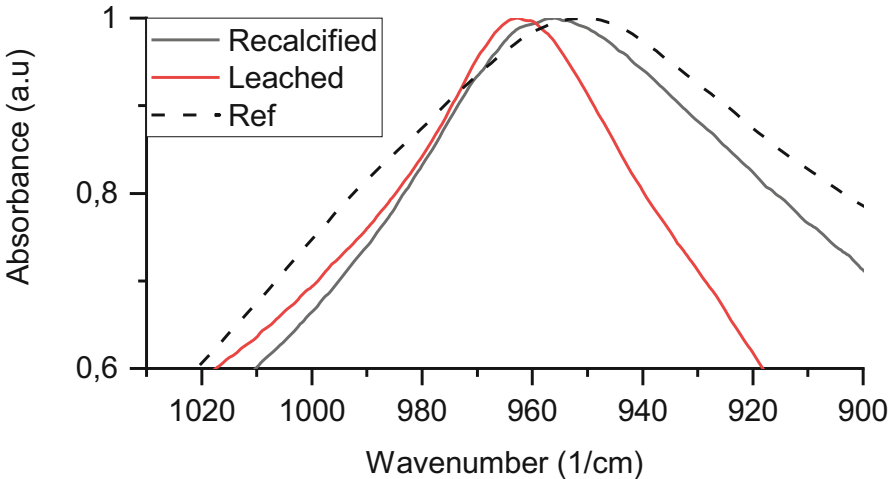


Fig. 4. Si-O asymmetric stretching (ν_3) in the degraded zone.

Recalcification not only recovers the Ca/Si ratio by integrating Ca^{2+} into deteriorated C-S-H, but it also has a pore-narrowing effect. Figure 5 depicts MIP intrusion data on reference, leached, and recalcified CEM I. The pore range of 50 nm to 1000 nm is primarily influenced by 6 days of recalcification. Figure 5a depicts the cumulative pore volume resulting from mercury intrusion. As shown in Table 1, the area under the leaching curve drops by 44% after 6 days of recalcification. There is also a modest decrease the in pore volume in the range of less than 50 nm, although MIP data of pore sizes smaller than 50 nm is not reliable owing to sample compression at high pressure. N_2 adsorption would deliver more trustworthy results in the region of small capillary and gel pores which is the subject of an ongoing study.

Figure 5b depicts the $dV/d\log D$ pore size distribution (PSD) curves of reference, leached, and recalcified CEM I. The pores in the reference sample are mostly located at approximately 50 nm in diameter, with one peak observed at that location. As leaching progresses, the 50-nm capillary pores widen, allowing the distribution from 100 to 1000 nm to appear. Along with the enlargement of capillary pores, gel pores with sizes less than 10 nm are also expected to shift to larger diameters. The peak about 20 nm is the result of gel-pore opening, which combines with the distribution from 100 to 1000 nm to form a 2-peak PSD curve, commonly seen in leached CEM I paste. As previously noted, recalcification has a pore filling effect in all pore diameters. However, such effect in the pore range of 100–1000 nm is most evident, with a dramatic drop in pores about

1000 nm (Fig. 5b). Due to recalcification, the PSD curve becomes more alike to that of the reference sample. The enlarged pores around 20 nm on the leaching PSD curve are likewise predicted to shrink as recalcification progresses, although N_2 adsorption is required to confirm such hypothesis.

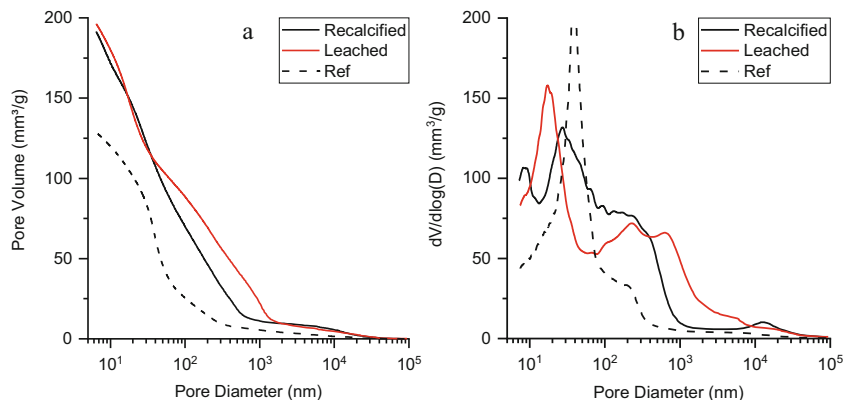


Fig. 5. (a) Cumulative pore volume derived from intruded volume of mercury and (b) pore size distribution of recalcified, leached and reference paste.

Table 1. Area under the cumulative pore volume curves, integrated from pore diameter of 50 nm to 1000 nm.

Area (mm ³ /g)	Ref	9546.4
	Leached	44903.0
	Recalcified	25206.2
Area reduction, recalcified vs. leached (%)		44

The pore filling effect of recalcification is visible under SEM images. The deteriorated zones in leached and recalcified paste are displayed in Fig. 6. The pores formed by calcium leaching in Fig. 6a are filled in Fig. 6b after recalcification. With a magnification of 20000 \times , a sponge-like network is observed in the spaces formed by leaching, as seen in Fig. 6d. This network is most likely C-S-H, either newly created or a result of the extension of degraded C-S-H owing to Ca^{2+} integration.

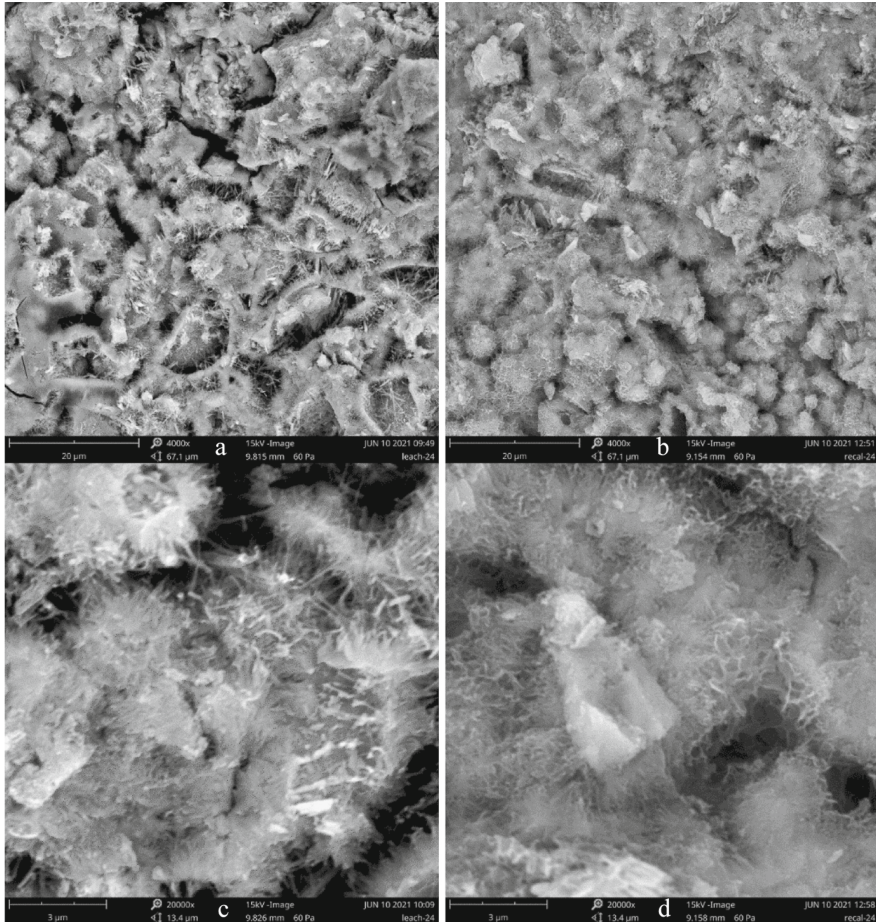


Fig. 6. SEM images of the degraded zone in leached (a, c) and recalcified (b, d) paste. The magnifications are 4000 times for (a, b) and 20000 times for (c, d).

4 Conclusions

Calcium leaching has been shown to be partially reversible. The pH of the deteriorated zone increases after 6 days of immersion in a saturated solution of $\text{Ca}(\text{OH})_2$, which together with an increase in the Ca/Si ratio indicates the presence of additional calcium in the damaged zone. Such incorporation of Ca^{2+} into the degraded paste is believed to be a chemical process – a hypothesis that is further supported by FTIR data of the Si-O ν_3 vibration. A red shift in peak position after recalcification is observed, which suggests a weakening of the Si-O bonds in the $[\text{SiO}_4]^{4-}$ polymeric units, or a shortening of the silicate chains.

Recalcification also exerts a pore filling effect, which reduces the volume of capillary pores and shifts the PSD of the leached paste to smaller pore diameters. In SEM, the substance that fills the leaching-formed pores has a sponge-like structure similar to that

of C-S-H. To confirm whether the observed phase is C-S-H or not, however, requires further studies on the leaching and recalcification of materials that contain only CH and C-S-H, i.e. hydrated C_3S paste.

The effects of recalcification on the chemistry and microstructure of a calcium-leached cement paste allow being employed in the healing of cementitious structures. Existing healing techniques concentrates on filling up cracks/voids with precipitates ($CaCO_3$, C-S-H or CH [14–17]) with little emphasis on the restoration of the deteriorated matrix. Recalcification can therefore be a beneficial addition, particularly when the structure in need of repair has already undergone Ca-degradation.

References

1. Phung, Q.T., Maes, N., Jacques, D., De Schutter, G., Ye, G.: Investigation of the changes in microstructure and transport properties of leached cement pastes accounting for mix composition. *Cem. Concr. Res.* **79**, 217–234 (2016). <https://doi.org/10.1016/j.cemconres.2015.09.017>
2. Segura, I., Molero, M., Aparicio, S., Anaya, J.J., Moragues, A.: Decalcification of cement mortars: Characterisation and modelling. *Cem. Concr. Compos.* **35**, 136–150 (2013). <https://doi.org/10.1016/j.cemconcomp.2012.08.015>
3. Chen, J.J., Thomas, J.J., Taylor, H.F.W., Jennings, H.M.: Solubility and structure of calcium silicate hydrate. *Cem. Concr. Res.* **34**, 1499–1519 (2004). <https://doi.org/10.1016/j.cemconres.2004.04.034>
4. Liu, L., Sun, C., Geng, G., Feng, P., Li, J., Dähn, R.: Influence of decalcification on structural and mechanical properties of synthetic calcium silicate hydrate (C-S-H). *Cem. Concr. Res.* **123**, 105793 (2019). <https://doi.org/10.1016/j.cemconres.2019.105793>
5. Thomas, J.J., Chen, J.J., Allen, A.J., Jennings, H.M.: Effects of decalcification on the microstructure and surface area of cement and tricalcium silicate pastes. *Cem. Concr. Res.* **34**, 2297–2307 (2004). <https://doi.org/10.1016/j.cemconres.2004.04.007>
6. Chen, J.J., Thomas, J.J., Jennings, H.M.: Decalcification shrinkage of cement paste. *Cem. Concr. Res.* **36**, 801–809 (2006). <https://doi.org/10.1016/j.cemconres.2005.11.003>
7. Carde, C., Escadeillas, G., François, A.H.: Use of ammonium nitrate solution to simulate and accelerate the leaching of cement pastes due to deionized water. *Mag. Concr. Res.* **49**, 295–301 (1997). <https://doi.org/10.1680/mac.1997.49.181.295>
8. Kamali, S., Gérard, B., Moranville, M.: Modelling the leaching kinetics of cement-based materials—influence of materials and environment. *Cem. Concr. Compos.* **25**, 451–458 (2003). [https://doi.org/10.1016/S0958-9465\(02\)00085-9](https://doi.org/10.1016/S0958-9465(02)00085-9)
9. Lea, F.M.: The action of ammonium salts on concrete. *Mag. Concr. Res.* **17**, 115–116 (1965). <https://doi.org/10.1680/mac.1965.17.52.115>
10. Varzina, A., Phung, Q.T., Perko, J., Jacques, D., Maes, N., Cizer, Ö.: Synergistic effects between carbonation and cracks in the hardened cement paste. *Sustainability* **14**, 8572 (2022). <https://doi.org/10.3390/su14148572>
11. Phung, Q.T.: Effects of carbonation and calcium leaching on microstructure and transport properties of cement pastes, dissertation. Ghent University (2015). <http://hdl.handle.net/1854/LU-6913935>. Accessed 23 Nov 2020
12. Phung, Q.T., Maes, N., Jacques, D., Schutter, G.D., Ye, G.: Decalcification of cement paste in NH_4NO_3 solution: microstructural alterations and its influence on the transport properties, vol. 9 (2019). ISBN 97890085787839
13. Acid-base indicators. <https://www.chemguide.co.uk/physical/acidbaseeqia/indicators.html>. Accessed 28 Nov 2022

14. Huang, H., Ye, G.: Self-healing of cracks in cement paste affected by additional Ca²⁺ ions in the healing agent. *J. Intell. Mater. Syst. Struct.* **26**, 309–320 (2015). <https://doi.org/10.1177/1045389X14525490>
15. Huang, H., Ye, G., Shui, Z.: Feasibility of self-healing in cementitious materials – by using capsules or a vascular system? *Constr. Build. Mater.* **63**, 108–118 (2014). <https://doi.org/10.1016/j.conbuildmat.2014.04.028>
16. De Belie, N., et al.: A review of self-healing concrete for damage management of structures. *Adv. Mater. Interfaces* **5**, 1800074 (2018). <https://doi.org/10.1002/admi.201800074>
17. Jonkers, H.M.: Self healing concrete: a biological approach. In: van der Zwaag, S. (ed.) *Self Healing Materials*, pp. 195–204. Springer, Dordrecht (2007). https://doi.org/10.1007/978-1-4020-6250-6_9